

## Amino acid analogues bind to carbon nanotube via $\pi$ - $\pi$ interactions: Comparison of molecular mechanical and quantum mechanical calculations

Zaixing Yang, Zhigang Wang, Xingling Tian, Peng Xiu, and Ruhong Zhou

Citation: *J. Chem. Phys.* **136**, 025103 (2012); doi: 10.1063/1.3675486

View online: <http://dx.doi.org/10.1063/1.3675486>

View Table of Contents: <http://jcp.aip.org/resource/1/JCPSA6/v136/i2>

Published by the [American Institute of Physics](#).

---

### Additional information on *J. Chem. Phys.*

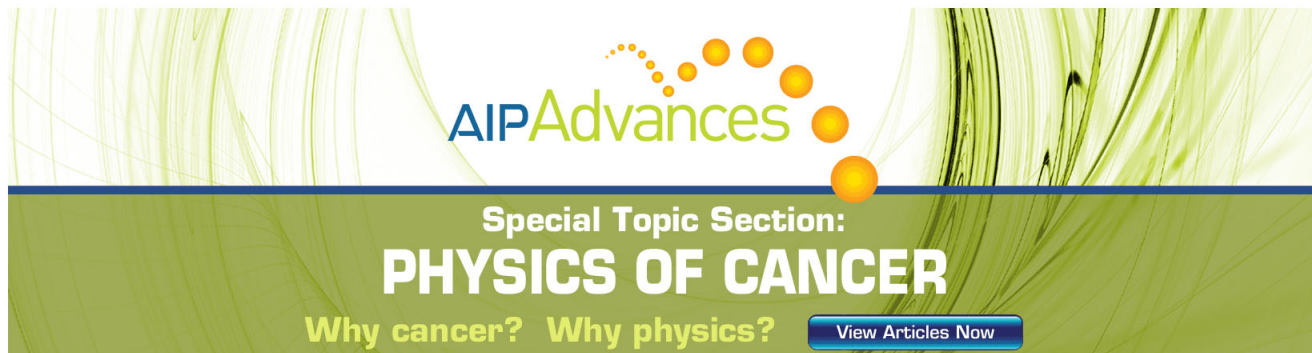
Journal Homepage: <http://jcp.aip.org/>

Journal Information: [http://jcp.aip.org/about/about\\_the\\_journal](http://jcp.aip.org/about/about_the_journal)

Top downloads: [http://jcp.aip.org/features/most\\_downloaded](http://jcp.aip.org/features/most_downloaded)

Information for Authors: <http://jcp.aip.org/authors>

## ADVERTISEMENT



**AIP Advances**

Special Topic Section:  
**PHYSICS OF CANCER**

Why cancer? Why physics? [View Articles Now](#)

# Amino acid analogues bind to carbon nanotube via $\pi$ - $\pi$ interactions: Comparison of molecular mechanical and quantum mechanical calculations

Zaixing Yang,<sup>1,2,a)</sup> Zhigang Wang,<sup>3,a)</sup> Xingling Tian,<sup>1</sup> Peng Xiu,<sup>1,2,b)</sup> and Ruhong Zhou<sup>4,b)</sup>

<sup>1</sup>Bio-X Lab, Department of Physics, and Soft Matter Research Center, Zhejiang University, Hangzhou 310027, China

<sup>2</sup>Department of Engineering Mechanics, Zhejiang University, Hangzhou 310027, China

<sup>3</sup>Institute of Atomic and Molecular Physics, Jilin University, Changchun 130012, China

<sup>4</sup>Computational Biology Center, IBM Thomas J. Watson Research Center, 1101 Kitchawan Road, Yorktown Heights, New York 10598, USA

(Received 12 September 2011; accepted 15 December 2011; published online 10 January 2012)

Understanding the interaction between carbon nanotubes (CNTs) and biomolecules is essential to the CNT-based nanotechnology and biotechnology. Some recent experiments have suggested that the  $\pi$ - $\pi$  stacking interactions between protein's aromatic residues and CNTs might play a key role in their binding, which raises interest in large scale modeling of protein-CNT complexes and associated  $\pi$ - $\pi$  interactions at atomic detail. However, there is concern on the accuracy of classical fixed-charge molecular force fields due to their classical treatments and lack of polarizability. Here, we study the binding of three aromatic residue analogues (mimicking phenylalanine, tyrosine, and tryptophan) and benzene to a single-walled CNT, and compare the molecular mechanical (MM) calculations using three popular fixed-charge force fields (OPLSAA, AMBER, and CHARMM), with quantum mechanical (QM) calculations using the density-functional tight-binding method with the inclusion of dispersion correction (DFTB-D). Two typical configurations commonly found in  $\pi$ - $\pi$  interactions are used, one with the aromatic rings parallel to the CNT surface (flat), and the other perpendicular (edge). Our calculations reveal that compared to the QM results the MM approaches can appropriately reproduce the strength of  $\pi$ - $\pi$  interactions for both configurations, and more importantly, the energy difference between them, indicating that the various contributions to  $\pi$ - $\pi$  interactions have been implicitly included in the van der Waals parameters of the standard MM force fields. Meanwhile, these MM models are less accurate in predicting the exact structural binding patterns (matching surface), meaning there are still rooms to be improved. In addition, we have provided a comprehensive and reliable QM picture for the  $\pi$ - $\pi$  interactions of aromatic molecules with CNTs in gas phase, which might be used as a benchmark for future force field developments.

© 2012 American Institute of Physics. [doi:10.1063/1.3675486]

## I. INTRODUCTION

Carbon nanotubes (CNTs) have recently become promising materials in various biological applications such as drug delivery,<sup>1</sup> tumor therapy,<sup>2</sup> biosensors,<sup>3</sup> and templates for biomolecule assembly.<sup>4</sup> However, there are still challenges facing the carbon nanotube industry, such as how to effectively disperse CNTs in solution, and how to assemble CNTs and other molecules into useful nano-structures. Some specific proteins/peptides have been proven to strongly bind to CNTs in experiments, thus can be used to disperse CNTs (Refs. 5–7) and potentially control their assembly.<sup>8</sup> Meanwhile, the wide biomedical applications raise the biosafety concerns of CNTs due to their unintended interactions with proteins and other biological molecules.<sup>9–13</sup> Therefore, a better understanding of the interactions of CNTs with biomolecules such as proteins and peptides is essen-

tial to CNT-based nanotechnology and biotechnology. Recent experiments have suggested that the proteins/peptides can bind to CNTs via hydrophobic interactions,<sup>4,5,7,8,14–16</sup>  $\pi$ - $\pi$  stackings,<sup>7,13,17–21</sup> electrostatic interactions (with the carboxylic defects on CNT),<sup>5,18</sup> and cation- $\pi$  interactions.<sup>6</sup> Among them, the  $\pi$ - $\pi$  stacking interactions between aromatic residues of protein/peptide and CNTs have been listed as a particularly important factor in the binding process.<sup>7,13,17–22</sup>

Given the importance of these complex interactions, there is a growing interest in recent years in modeling the protein/peptide-CNT interactions using molecular dynamics (MD) simulations. Most of them are based on atomistic simulations with fixed-charge (nonpolarizable) force fields;<sup>11–13,23–31</sup> others are based on atomistic simulations with polarizable force field,<sup>32,33</sup> or coarse-grained MD simulations.<sup>26,30,34</sup> Consistent with the experiments, several MD studies support the crucial role of  $\pi$ - $\pi$  stacking interactions in peptide/protein-CNT binding.<sup>11–13,24–26,32,33</sup> Compared to the quantum mechanical (QM) methods, the MD simulations can significantly reduce the computational cost and thus allow simulations of systems with a large

<sup>a)</sup>Z. Yang and Z. Wang contributed equally to this work.

<sup>b)</sup>Author to whom correspondence should be addressed. Electronic addresses: xiupeng2011@zju.edu.cn and ruhongz@us.ibm.com.

number of atoms.<sup>35–40</sup> However, the  $\pi$ - $\pi$  interactions are the interactions between  $\pi$ -electron systems (interaction between the parallel  $\pi$ -systems is specially termed as “ $\pi$ - $\pi$  stacking interaction”) and are traditionally explored with QM approaches.<sup>41–51</sup> It is fascinating that the negatively charged and diffuse electron clouds of the  $\pi$ -systems exhibit an attractive interaction. The high-level QM calculations of benzene dimer provided useful insights about the dominant factors of  $\pi$ - $\pi$  interactions, which include dispersion, electrostatic (quadrupole-quadrupole and CH- $\pi$  interactions), and exchange-repulsion interactions, with the dispersion interaction serving as the major source of attraction.<sup>41–46</sup> On the other hand, for molecular mechanical (MM) approach, previous reports<sup>52–55</sup> indicated that the standard (fixed-charge) force fields can properly model the  $\pi$ - $\pi$  interactions of benzene dimer partly due to the fact that the partial charges on benzene molecule in these force fields accurately reproduce benzene’s quadrupole moment,<sup>56</sup> and hence can properly treat the electrostatic interactions between benzene dimer (see Refs. 52 and 54, and Table S1 in the supplementary material (Ref. 82)). However, the atoms of CNT are usually modeled as uncharged Lennard-Jones particles in standard MM force fields. In these cases, the interactions, including  $\pi$ - $\pi$  (stacking) interactions, between protein/peptide and CNT reduce to van der Waals (vdW) terms only; that is, the electrostatic interactions between aromatic residue and permanent multipoles of CNT’s aromatic rings (due to  $\pi$ -electron clouds on aromatic rings) as well as the induced polarizability are not taken into account. Therefore, some may naturally infer that MD simulations with fixed-charge force fields might yield a significant underestimation of the  $\pi$ - $\pi$  (stacking) interactions, thus inappropriate for studying the aromatic residues-CNT interactions.<sup>32,33</sup> The validation of these models with MM approach is thus highly needed for the studies of protein/peptide-CNT interactions, in view of the key role that the  $\pi$ - $\pi$  stacking interactions play in protein/peptide-CNT binding. To our knowledge, such validation is not yet available in literature. Moreover, even though there are a few QM studies on the interaction of amino acid analogues (or peptide) with CNTs,<sup>32,57–60</sup> and some of them highlighted the importance of  $\pi$ - $\pi$  stacking,<sup>32,60</sup> a systematic and reliable description of the  $\pi$ - $\pi$  stacking between aromatic residues and CNT is still missing. Some of earlier QM approaches<sup>57,58</sup> also gave very poor results on the  $\pi$ - $\pi$  stacking interactions of amino acids with CNT when compared to experiments.

In this study, we investigate the binding of analogues of three aromatic amino acids [i.e., using a methyl group to replace the backbones of phenylalanine (Phe), tyrosine (Tyr), and tryptophan (Trp); for simplicity, we use the same abbreviations Phe, Tyr, and Trp in the following] and benzene to the outer surface of a single-walled CNT in gas phase via  $\pi$ - $\pi$  interactions with both QM and MM approaches. We are interested in these aromatic amino acids, since their  $\pi$ - $\pi$  stacking interactions with nanotubes have been shown experimentally to play a key role in the adsorption of proteins/peptides onto CNTs.<sup>7,13,17–22</sup> Although histidine (His), whose side chain has an aromatic ring as well, is also found to play an important role in peptide-CNT binding in some cases,<sup>7</sup> we do not consider it here since it may compli-

cate the situation by bringing another class of interaction, the cation- $\pi$  interaction, into play. The benzene-CNT interactions, the simplest prototype of  $\pi$ - $\pi$  interactions between aromatic molecules and CNT, are also studied as a “benchmark”. We adopt the density-functional tight-binding (DFTB) method with the inclusion of dispersion correction (acronym DFTB-D)<sup>61–63</sup> for QM calculations, and three most commonly used fixed-charge force fields, namely, OPLSAA,<sup>64</sup> AMBER,<sup>65</sup> and CHARMM,<sup>66</sup> for MM calculations. We consider two configurations which are energetically favorable and commonly used for the study of  $\pi$ - $\pi$  interactions,<sup>32,42–44</sup> with the aromatic rings parallel or perpendicular to the CNT surface (see Fig. 2). For the binding interaction energies, the MM data for both configurations as well as their energy differences are very comparable with the referenced QM data, indicating that the various contributions to  $\pi$ - $\pi$  interactions have been implicitly included in the vdW parameters of the standard MM force fields. On the other hand, however, for the equilibrium structures of aromatic molecule-CNT complexes, the MM and QM predictions are somewhat different. These results indicate that although the MM approaches may be incapable of accurately predicting the exact binding structures (patterns), they can yield reasonably satisfactory descriptions of the strength of  $\pi$ - $\pi$  interactions between aromatic molecules and CNT, which is often the most important aspect in the study of aromatic amino acids-CNT interactions. Together, our study not only demonstrates the capability of MD simulations with fixed-charge force fields in describing the  $\pi$ - $\pi$  interactions, which is critical for the MD studies of protein/peptide-CNT interactions, but also provides a comprehensive and reliable QM picture for the  $\pi$ - $\pi$  interactions of aromatic molecules with CNTs in gas phase, which might be used as a benchmark for future force field developments.

## II. METHODS

It should be noted that even QM methods have difficulty in properly modeling  $\pi$ - $\pi$  interactions, because many of them ignore the London dispersion forces which are caused by favorable instantaneous multipole/induced multipole charge fluctuations.<sup>45</sup> Hartree-Fock molecular orbital theory describes the motion of each electron in the average field of the other electrons, so it is incapable of describing the instantaneous correlated motions of electrons which give rise to dispersion forces.<sup>45</sup> Although the post-Hartree-Fock methods [such as MP2 and CCSD(T) (coupled cluster theory including single, double, and perturbative triple excitations)] are considered as standard methods to treat the dispersion force, they are practically inapplicable to large biomolecular systems due to their expensive computational costs. It is also known that the conventional density functional theory (DFT) methods are inherently very deficient for stacking interactions as they basically ignore the dispersion attraction.<sup>67</sup> Alternatively, augmenting the conventional DFT methods by an empirical dispersion term (DFT-D) appears to be a reasonable way to improve the major deficiency of a DFT method for investigating molecular systems with  $\pi$ - $\pi$  stacking interactions.<sup>47,59,68</sup> In this study, we used the density-functional tight-binding method,<sup>61,62</sup> with the inclu-

sion of dispersion correction.<sup>63</sup> The DFTB method is a computationally efficient approximation to DFT method, which is based on a second-order expansion of the Kohn-Sham total energy in DFT with respect to charge density fluctuations. In general, it closely approximates DFT but runs  $\sim 10^3$  to  $10^4$  times faster.<sup>61</sup> The DFTB-D method has been proven to be successful in treating  $\pi$ - $\pi$  stacking interactions between nucleic acid base pairs<sup>63</sup> and has already been used to study the binding of peptides to CNT.<sup>60</sup>

To further assess the reliability of DFTB-D method for the current study, we take the benzene dimer and indole-benzene complex as model systems, and compare our current DFTB-D results against those of other QM methods [CCSD(T), QCISD(T) (singles and doubles quadratic configuration interaction with a perturbative treatment of triple substitution), MP2, DFT-D, and another version of DFTB-D (Ref. 69) (denoted by DFTB-D\*), MM force fields, and the experiments. Some comparisons are presented in Table I, and a complete list of comparison can be found in the supplementary material.<sup>82</sup> In case of benzene dimer, four most commonly investigated configurations are considered (see Fig. 1). Among them, the PD and TT ones are almost isoenergetic and currently viewed as the most stable configurations of benzene dimer;<sup>42,43</sup> they correspond to the “flat” and “edge” configurations of aromatic molecule-CNT complex, respectively. From Table I, we can see that the DFTB-D yields fairly reasonable interaction energies as compared to CCSD(T) calculations (especially for PD and TT configurations, which

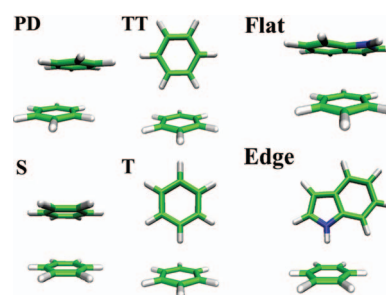


FIG. 1. Investigated configurations of model aromatic complexes. For benzene dimer (left), four configurations are considered: parallel-displaced  $C_{2h}$  (PD), T-shaped tilted  $C_s$  (TT), sandwich  $D_{6h}$  (S), and T-shaped  $C_{2v}$  (T). For indole-benzene complex (right), two configurations are considered: parallel-displaced (flat) and T-shaped (edge).

are the most important configurations for the current study, but for the S configuration the difference is slightly larger), and in most cases, it seems even superior to standard MP2 treatments [even at the complete basis set (CBS) limit of MP2 level], which often overestimate the interactions. Also, the DFTB-D energies for TT and T configurations ( $-2.36$  and  $-2.08$  kcal/mol, respectively) are in good agreement with the experimentally determined dissociation energy of the gas phase T-shape-like benzene dimer ( $2.4 \pm 0.4$  kcal/mol).<sup>70</sup> In addition, we have built another system with a benzene molecule on top of a graphene; the DFTB-D predicted interaction energy between them is  $-10.0$  kcal/mol, which is in good agreement with the measured heat of adsorption of benzene on graphitized carbon black ( $-9.4$  kcal/mol).<sup>71</sup>

In case of benzene-indole complex, we only consider the flat and edge configurations (see Fig. 1), for which the benchmark calculations [CCSD(T)] are available in literature. Similar to the case of benzene dimer, DFTB-D method yields very reasonable interaction energies as compared to CCSD(T) calculations (especially for flat configuration), and it can be even more accurate than the MP2 calculations (see Table I).

To test the reliability of DFTB-D method for geometry prediction, we have compared equilibrium distance of benzene dimer with different configurations predicted by DFTB-D against those of other QM methods, standard MM force fields, and experiment (some comparisons are presented in Table II, and a complete list of comparison can be found in the supplementary material).<sup>82</sup> There are several interesting findings. First, as compared to the experimental<sup>72</sup> and CCSD(T) references, the DFTB-D method slightly underestimates the equilibrium distances (by  $0.25$  Å and  $0.13$  Å, for PD and T configurations, respectively; consistent with the results of interaction energy, the error for S configuration is slightly larger). It is also noteworthy that for PD configuration, the DFTB-D result is very close to those of MP2/aug-cc-pVQZ and MP2/TZ-CP. Second, equilibrium distances of standard MM force fields agree quite well with CCSD(T) predictions for PD configuration (see CHARMM case of Table S3 in supplementary material) (Ref. 82) but with slight differences for S and T configurations. Last, we would like to compare the reliability of the two DFTB methods, both of which are within the DFTB framework, for studying  $\pi$ - $\pi$  interactions. As compared to the DFTB-D method, DFTB-D\* seems to work slightly better in predicting the equilibrium distances

TABLE I. Comparison of interaction energies (kcal/mol) of benzene dimer (A) and benzene-indole complex (B) obtained by different quantum mechanical (QM) methods.

Methods	(A) Benzene dimer			
	PD	TT	S	T
CCSD(T) <sup>a</sup>	-2.70	-2.78	-1.64	-2.69
DFTB-D <sup>b</sup>	-3.19	-2.36	-3.13	-2.08
DFTB-D* <sup>c</sup>	-4.37	-2.83	-4.38	-2.53
MP2/aug-cc-PVTZ <sup>d</sup>	-4.25	-2.83	-2.87	-3.22
MP2/aug-cc-pVQZ <sup>e</sup>	-4.73	...	-3.35	-3.48
MP2/CBS <sup>f</sup>	-4.95	...	...	-3.62

Methods <sup>g</sup>	(B) Benzene-indole complex	
	Flat	Edge
CCSD(T)	-5.22	-5.73
DFTB-D	-4.66	-4.23
DFTB-D*	-6.03	-4.09
MP2/aug-cc-PVTZ	-7.36	-6.29
MP2/CBS	-8.12	-7.03

<sup>a</sup>High-level CCSD(T) interaction energies.<sup>43</sup>

<sup>b</sup>DFTB-D energies with the standard approach to treat dispersion correction (using  $R^{-6}$  term).

<sup>c</sup>DFTB-D\* energies calculated with another version of DFTB-D method whose dispersion correction adopts the Lennard-Jones 6-12 potential (with short-range repulsion term corrected by a polynomial function) and vdW parameters of universal force field (UFF).<sup>69</sup>

<sup>d</sup>Energies calculated at MP2/aug-cc-PVTZ level with basis set superposition error correction, see the corresponding footnote of Table S2 in the supplementary material for details.<sup>82</sup>

<sup>e</sup>MP2 energies with a modified aug-cc-pVQZ basis.<sup>45</sup>

<sup>f</sup>MP2 complete basis set limit energies for S22 set.<sup>48</sup>

<sup>g</sup>CCSD(T) data in this table derive from the CCSD(T) CBS limit interaction energies for S22 set.<sup>48</sup> The description of other methods can be found in the methods discussed for benzene dimer (A).

TABLE II. Comparison of equilibrium distances (Å) of benzene dimer obtained by different methods.<sup>a</sup>

Methods	PD	TT	S	T
Experiment <sup>b</sup>	...	...	...	4.96
CCSD(T) <sup>c</sup>	3.6	...	3.9	5.0
DFTB-D	3.35	4.71	3.43	4.83
DFTB-D <sup>*d</sup>	3.47	4.99	3.55	5.16
MP2/6-31g <sup>**e</sup> (0.25, 0.15) <sup>e</sup>	3.16	4.81	3.52	4.71
MP2/aug-cc-pVQZ <sup>f</sup>	3.4	...	3.7	4.9
MP2/TZ-CP <sup>g</sup>	3.36	...	...	4.91

<sup>a</sup>The distance is defined as the vertical distance between geometrical centers of benzene dimer.

<sup>b</sup>See Ref. 72.

<sup>c</sup>High-quality estimates of CCSD(T) results with a modified aug-cc-pVQZ basis.<sup>49</sup>

<sup>d</sup>DFTB-D<sup>\*</sup> denotes another version of DFTB-D method, see the footnote of Table IA.

<sup>e</sup>Distances calculated by us at MP2/6-31g<sup>\*\*</sup> (0.25, 0.15) level, see supplementary material for details.<sup>82</sup>

<sup>f</sup>See Ref. 49.

<sup>g</sup>Distances calculated by us using the geometry which is obtained by Hobza *et al.*<sup>48</sup> at MP2/cc-pVTZ level with the counterpoise corrected gradient optimization.

but yields poorer results in predicting interaction energies in most cases [in particular, DFTB-D<sup>\*</sup> significantly overestimates the energies of stacked configuration in both benzene dimer and benzene-indole complex cases (see Table I)]. In our current applications, an accurate prediction of interaction energy is probably more important, therefore, we have chosen the DFTB-D rather than the DFTB-D<sup>\*</sup>, as the QM method in our study of the aromatic molecules-CNT interactions.

In case of MM calculations, the GROMACS 4.5.3 software<sup>73</sup> was used, with the VMD software<sup>74</sup> to view the trajectories and draw molecular pictures. Parameters for the amino acid analogues derived from three most commonly used fixed-charge force fields, namely, OPLSAA,<sup>64</sup> AMBER (AMBER99),<sup>65</sup> and CHARMM (a modified version of CHARMM22 force field).<sup>66</sup> The carbon atoms of CNTs were modeled as uncharged Lennard-Jones particles with a cross-section of  $\sigma_{cc} = 0.34$  nm and a depth of the potential well of  $\epsilon_{cc} = 0.3598$  kJ mol<sup>-1</sup>.<sup>75-77</sup> The vdW interaction are described with the Lennard-Jones 6-12 potential, using the geometric combination rule for vdW parameters of OPLSAA force field, and Lorentz-Bertelot combination rule for CHARMM and AMBER force fields. Some other detailed treatments of vdW parameters of amino acid analogues are present in the supplementary material.<sup>82</sup>

In MM calculations, an energy minimization is usually used to optimize the initial structure. However, the energy minimization is mainly used to avoid excessively large forces in the crystal structure with bad contacts, and is most likely to be trapped in local minima of the potential energy landscape. Therefore, this method alone is unable to explore the optimal binding structures and the corresponding interaction energies. Searching and mapping the landscapes of interaction energy between aromatic molecules and CNT are thus needed. We introduced the following procedure: the initial structures for MM calculations were taken from the QM equilibrium structures; then the aromatic molecules were scanned/optimized along three different reaction coordinates, namely,  $d$ ,  $\phi$ , and  $\psi$  (see Fig. 3(a)):  $d$  is defined as the distance between geometrical centers of molecule's aromatic ring and CNT surface,

covering the range of physisorption distances;  $\phi$  represents the "autorotation" of the aromatic ring, defined as the angle of the aromatic ring anti-clockwise rotating against the ring normal axis; and  $\psi$  represents the "revolution" of the aromatic ring relative to CNT, defined as the angle of the aromatic ring anti-clockwise rotating against the long axis of CNT. Given the symmetry of (5, 5) CNT, the ranges of both  $\phi$  and  $\psi$  are from 0° to 90°. At each coordinate of ( $d$ ,  $\phi$ ,  $\psi$ ), the energy of system was minimized with a steepest descent algorithm, and then the interaction energy was computed. Last, the global minimum in interaction energy landscape and its corresponding structure are considered as the interaction energies of binding and the equilibrium structure for this aromatic molecule.

### III. RESULTS AND DISCUSSION

A 250-carbon, hydrogen-terminated, (5, 5) armchair nanotube (29.4 Å in length and 6.8 Å in diameter) was aligned along the z axis with its positions restrained (fixed in space) in both MM and QM calculations. Initially, the aromatic molecules were placed above the outer surface of the CNT at physisorption distances with their aromatic rings oriented parallel and perpendicular to the CNT surface, respectively, forming a "flat" (face-to-face) and an "edge" (edge-to-face) configuration (see Fig. 2). There are two reasons for our choice of the two configurations: First, they are commonly used for the study of  $\pi$ - $\pi$  interactions.<sup>32,42-44</sup> From the QM view, the two configurations enable the  $\pi$ - $\pi$  stacking and the electrostatic interactions of hydrogens on aromatic ring with  $\pi$  electrons of CNT (the CH- $\pi$  interaction), respectively, thus energetically favorable. Second, several MD simulations found that the aromatic residues adsorbed onto CNTs adopted both the "flat"<sup>11-13,24,25,32,33</sup> and "edge"<sup>11,13,24,33</sup> configurations, with the "flat" one predominant.

Unlike the previous works<sup>32,46</sup> that the QM and MM calculations of interaction energies are based on the same structure, in the current study, QM and MM approaches follow different procedures to search their respective optimal structures. In case of QM calculations, for both "flat" and "edge" configurations, a series of initial arrangements were used to search the optimal structure. We found several stable structures for the "flat" configuration, with their energy difference in the order of 0.1 kcal/mol. The most stable structure (with minimal interaction energy) is then considered as the optimal (equilibrium) structure. In case of MM calculations, we mapped the interaction energy landscapes along three reaction coordinates to obtain the minimal interaction energies and optimal structures (see Sec. II for details). Figure 3 shows the

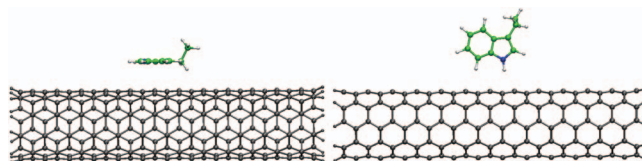


FIG. 2. Initial arrangements of the system (side view), using the tryptophan analogue for illustration. Left and right panels show "flat" and "edge" configurations, with the aromatic rings parallel and perpendicular to the carbon nanotube (CNT) surface, respectively. The CNT used here is a hydrogen-terminated (5,5) armchair nanotube.

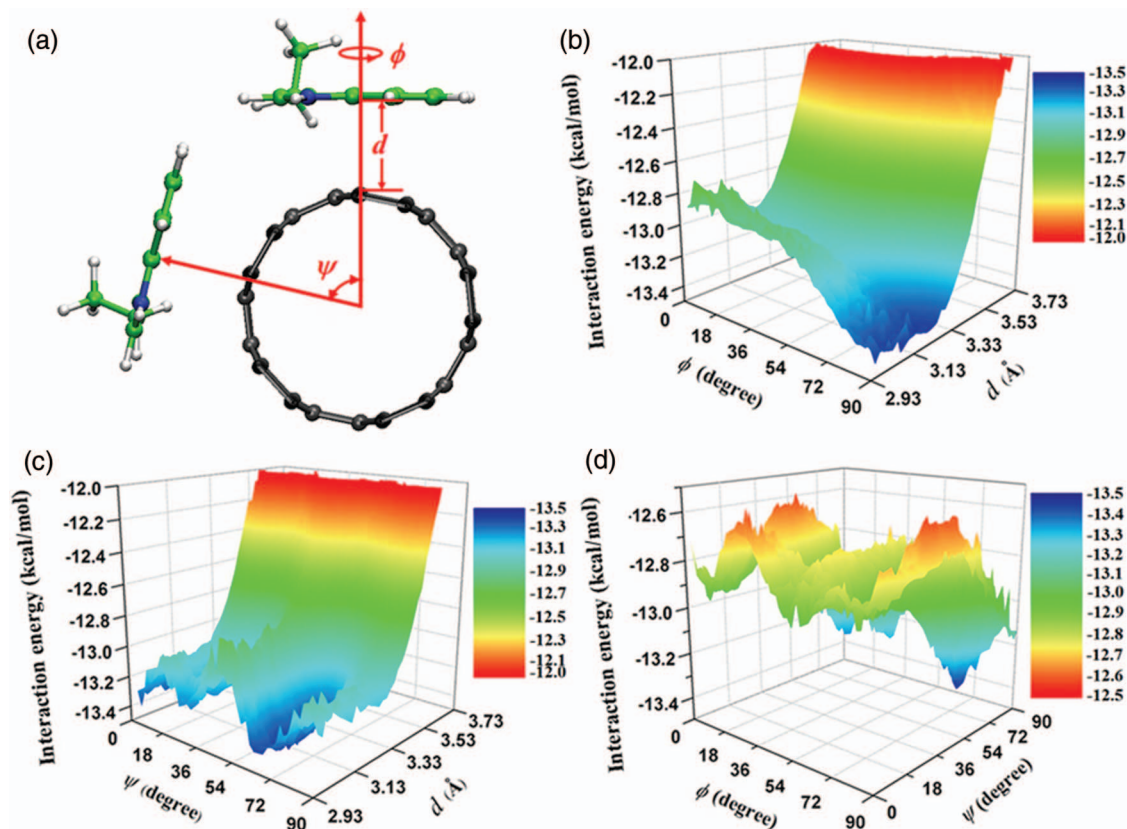


FIG. 3. Mapping the interaction energy landscapes for aromatic molecule-CNT complexes with molecular mechanical (MM) calculations, using tryptophan analogue with “flat” configuration and AMBER force field for illustration. (a) Schematic representation of three reaction coordinates used for mapping interaction energy landscapes.  $d$ ,  $\phi$ , and  $\psi$ , where  $d$  is the ring-CNT distance, and  $\phi$  and  $\psi$  are the angles of aromatic ring rotating along the surface normal and CNT axis, respectively. (b–d) Interaction energy (in kcal/mol) landscapes with three different pairs of reaction coordinates ( $d$ ,  $\phi$ ), ( $d$ ,  $\psi$ ), and ( $\phi$ ,  $\psi$ ), respectively. For each landscape, the third reaction coordinate is kept at the optimal position of the final equilibrium structure.

interaction energy landscapes, using the Trp with “flat” configuration for AMBER case as an example. We find that the interaction energies between aromatic molecules and the CNT are very sensitive to the molecule-CNT distance (Figs. 3(b) and 3(c)), and somewhat dependent on the  $\phi$  and  $\psi$  angles (Fig. 3(d)), the “autorotation” angle of the aromatic ring, and the “revolution” angle of molecule with respect to the CNT surface, respectively.

Table III compares the QM and MM interaction energies of binding for the four aromatic molecules with both “flat” and “edge” configurations as well as their energy differences, denoted as  $\Delta E_{\text{flat}}$ ,  $\Delta E_{\text{edge}}$ , and  $\Delta\Delta E$ , respectively. We find that MM results show very good agreements with the corresponding QM data, with the majority showing an energy difference of less than 1 kcal/mol, and the agreement is particularly excellent for the benzene molecule. The small exceptions are in  $\Delta E_{\text{flat}}$  for Tyr predicted by OPLSAA and AMBER force fields (differ by  $-1.17$  and  $-1.64$  kcal/mol, respectively), and in  $\Delta\Delta E$  for AMBER Tyr (differs by a value of  $-1.19$  kcal/mol). We note that overall the MM calculations show a slight overestimate of the interaction energies as compared to QM results, with the AMBER case showing the most noticeable overestimation. Nevertheless, the general good agreement between MM and QM data is very encouraging, and perhaps even surprising and unexpected to some researchers, because of the classical treat-

ments of the  $\pi$ - $\pi$  interactions and the simple forms of potential functions (i.e., no polarizability) in the MM approach. This striking agreement indicates that, although some interactions, e.g., the electrostatic interactions between aromatic molecules and CNTs [the polarizability is negligible (see below)]; but in general, the electrostatic interactions between

TABLE III. Comparison of QM and MM calculated interaction energies (kcal/mol) of binding for aromatic molecules.<sup>a</sup>

Binding energy		DFTB-D	OPLSAA	AMBER	CHARMM
Phe	$\Delta E_{\text{flat}}$	-9.63	-9.71	-10.04	-9.73
	$\Delta E_{\text{edge}}$	-6.34	-6.86	-6.48	-6.93
	$\Delta\Delta E$	-3.28	-2.85	-3.56	-2.80
Tyr	$\Delta E_{\text{flat}}$	-9.77	-10.94	-11.41	-10.74
	$\Delta E_{\text{edge}}$	-5.71	-6.51	-6.16	-6.59
	$\Delta\Delta E$	-4.06	-4.43	-5.25	-4.15
Trp	$\Delta E_{\text{flat}}$	-12.68	-12.85	-13.47	-13.21
	$\Delta E_{\text{edge}}$	-6.39	-6.55	-6.35	-6.73
	$\Delta\Delta E$	-6.29	-6.30	-7.12	-6.48
Benzene	$\Delta E_{\text{flat}}$	-7.59	-7.87	-8.17	-8.02
	$\Delta E_{\text{edge}}$	-4.00	-4.54	-4.10	-4.54
	$\Delta\Delta E$	-3.59	-3.33	-4.07	-3.48

<sup>a</sup>  $\Delta E_{\text{flat}}$  and  $\Delta E_{\text{edge}}$  denote the interaction energies of binding for “flat” and “edge” configurations, respectively, and  $\Delta\Delta E$  denotes the energy difference between them. The abbreviations of amino acid analogues are the same as the corresponding amino acids.

aromatic molecules and permanent multipoles of CNT's aromatic rings can not be ignored] are not explicitly treated, their contributions have been implicitly incorporated into the vdW interactions. Moreover, it is noteworthy that in comparison with the OPLSAA and CHARMM cases, the AMBER interaction energies are relatively low for the "flat" configuration but relatively high for the "edge" configuration. Remarkably, the magnitude of all  $\Delta E_{\text{flat}}$  values of aromatic residues analogues are in the order of 10 kcal/mol ( $\sim 17$  k<sub>B</sub>T), indicating strong aromatic residues-CNT binding. More interestingly, both QM and MM calculations indicate that the rank order (from strong to weak) of the strength of  $\pi$ - $\pi$  stacking interaction with the CNT for three aromatic residues analogues is Trp, Tyr, and Phe, which is same as that obtained experimentally by Xie *et al.*,<sup>19</sup> and consistent with many other experimental<sup>7,18-21</sup> and computational<sup>11,12,24,32,33,60</sup> observations that the tryptophan plays a particular important role in the protein and peptides' binding to CNT.

Next, we discuss some implications of the QM data in Table III. First, we know that apart from  $\pi$ - $\pi$  interactions, there are other interactions existing in the system, such as the dispersion and CH- $\pi$  interactions<sup>60</sup> between aliphatic groups (CH<sub>2</sub> and CH<sub>3</sub>) and CNT. However, these interactions are found to be much weaker than the  $\pi$ - $\pi$  interactions, by comparing the QM interaction energies of Phe-CNT with those of benzene-CNT. Hence, the binding of amino acid analogues to CNT is dominated by the  $\pi$ - $\pi$  interactions. Second,  $\Delta E_{\text{flat}}$  is found to be always lower than the corresponding  $\Delta E_{\text{edge}}$ , indicating that the "flat" configuration, which can enable  $\pi$ - $\pi$  stacking interactions, is energetically more favorable than the "edge" one. This finding is in contrast to the case of benzene dimer, where the "edge" configuration (TT) is slightly more stable than the "flat" one (PD) (binding energy lower by  $\sim 0.1$  kcal/mol).<sup>42,43</sup> This discrepancy is due to the fact that in the present case (aromatic molecules interacting with CNT rather than a benzene molecule), the "flat" configuration can facilitate the aromatic molecules to effectively interact with many more carbon atoms on CNT (not just the "benzene ring" facing it) via dispersion interactions than the "edge" one. In other words, the CNT has many more carbon atoms than a benzene molecule, so the dispersion interaction will play an even more significant role in the present case than in benzene dimer case, which can also be seen from the much lower binding affinities for the benzene dimer,  $-2.70$  kcal/mol for the "flat" (PD) configuration and  $-2.78$  kcal/mol for the "edge" (TT) one.<sup>43</sup> Last, it should be emphasized the importance of dispersion correction for the DFT (including DFTB) calculations of  $\pi$ - $\pi$  stacking interaction. A previous report<sup>78</sup> on a benzene molecule adsorbed onto a (5, 5) CNT using DFT method at local density approximation (LDA) level (i.e., DFT-LDA that does not include the dispersion correction) gave a value of  $-4.45$  kcal/mol in interaction energy, which is significantly weaker than our DFTB-D result ( $-7.59$  kcal/mol) (some discussions on the reliability of DFTB-D method is presented in METHODS). Moreover, the QM calculations using DFT-LDA method by Walsh and Tomasio<sup>32</sup> showed that the "flat" and "edge" configurations of benzene-CNT complex have exactly the same binding energy. This evidently incorrect conclusion should originate from the underestimate of

the dispersion, particularly for the "flat" configuration. Likewise, it is well known that the DFT method at generalized-gradient approximations level usually tends to underestimate the interaction between  $sp^2$ -like materials.<sup>78,79</sup> Hence, we emphasize that when calculating the  $\pi$ - $\pi$  stacking interactions between aromatic molecules and CNT, it is necessary to introduce the dispersion correction to conventional DFT method, otherwise, a significantly underestimated stacking interaction will be yielded in QM calculations.

As mentioned above, in the previous works,<sup>32,46</sup> the QM and MM calculations of  $\pi$ - $\pi$  interaction energies are based on the same QM structure. Thus, one may wonder how the interaction energies change in our case if we use the same QM structure for MM calculations. Table IV lists the results ["MM (before Minimization)" section]. Remarkably, all MM data of  $\Delta E_{\text{flat}}$  are significantly higher than the QM data ( $\Delta E_{\text{edge}}$  and  $\Delta\Delta E$  are higher than the corresponding QM data as well; note that the OPLSAA and CHARMM data of  $\Delta\Delta E$  are positive), consistent with the suggestion by Sherrill *et al.*<sup>46</sup> that if the calculations are based on the same structure, MM calculations of  $\pi$ - $\pi$  interactions cannot reproduce the corresponding QM data. The significant underestimates of the  $\pi$ - $\pi$  interactions are due to the fact that the equilibrium ring-CNT distances predicated by QM calculations are smaller than those of MM calculations (see Table V below), giving rise to repulsive forces between aromatic molecules and CNT. If the QM equilibrium structures are slightly adjusted by energy minimization procedures in MM approach (see Sec. II), the resulting MM data appear to largely agree with the QM data with the exception of  $\Delta E_{\text{flat}}$  in CHARMM case, as shown in "MM (after Minimization)" section of Table IV. However, these MM results of  $\Delta E_{\text{flat}}$  and  $\Delta E_{\text{edge}}$  remain relatively weaker than those in Table III, indicating that it is necessary to search for MM's own global minimum, and that equilibrium structures obtained by QM and MM calculations are not the same (more below).

One may be wondering what kind a role the polarizability plays in the current aromatic molecule-CNT binding. To address this question, we have calculated the maximal induced charges (Mulliken charges determined by DFTB-D calculations) on atoms of CNT, and the induced "polarization energy" (Coulomb interaction energy between the induced charges of CNT and aromatic molecules). As shown in Table V, both the atomic induced charges (with the largest one less than 0.017 e) and the induction energies are negligible, suggesting that the CNT polarizability due to aromatic rings is insignificant, thus, the polarizable force fields might be unnecessary for studying  $\pi$ - $\pi$  interactions in this case.

In addition to the interaction energies of binding, we also compare the QM and MM predicted equilibrium structures. We find that in both QM and MM cases, the aromatic rings of molecules in equilibrium structures remain nearly parallel and perpendicular to CNT, for the "flat" and "edge" configurations, respectively (all QM predicted structures shown in side view are presented in the supplementary material).<sup>82</sup> Given the importance of  $\pi$ - $\pi$  stacking interaction, here we only discuss the results for the "flat" configuration in detail (shown in Fig. 4 and Table VI), and the results for the "edge" case are presented in the supplementary material.<sup>82</sup> First, we focus on

TABLE IV. Comparison of QM and MM calculated interaction energies (in kcal/mol) between aromatic molecules and CNTs based on the equilibrium structures predicted by QM calculations.<sup>a</sup>

Binding energy	QM	MM (before minimization) <sup>b</sup>			MM (after minimization) <sup>c</sup>			
		DFTB-D	OPLSAA	AMBER	CHARMM	OPLSAA	AMBER	CHARMM
Phe	$\Delta E_{\text{flat}}$	-9.63	-5.67	-6.49	-5.98	-8.83	-9.51	-7.71
	$\Delta E_{\text{edge}}$	-6.34	-6.00	-5.54	-6.02	-6.69	-6.41	-6.40
	$\Delta \Delta E$	-3.28	0.33	-0.95	0.04	-2.14	-3.14	-1.31
Tyr	$\Delta E_{\text{flat}}$	-9.77	-6.41	-7.69	-6.48	-9.93	-10.74	-8.19
	$\Delta E_{\text{edge}}$	-5.71	-5.09	-4.04	-4.60	-6.32	-6.04	-5.75
	$\Delta \Delta E$	-4.06	-1.32	-3.65	-1.88	-3.61	-4.70	-2.44
Trp	$\Delta E_{\text{flat}}$	-12.68	-7.43	-8.79	-9.58	-12.21	-12.84	-11.31
	$\Delta E_{\text{edge}}$	-6.39	-5.99	-5.53	-5.95	-6.29	-6.13	-6.34
	$\Delta \Delta E$	-6.29	-1.44	-3.26	-3.63	-5.92	-6.71	-4.97
Benzene	$\Delta E_{\text{flat}}$	-7.59	-6.27	-7.22	-6.40	-7.52	-7.98	-6.81
	$\Delta E_{\text{edge}}$	-4.00	-3.68	-2.79	-3.32	-3.78	-3.04	-3.65
	$\Delta \Delta E$	-3.59	-2.59	-4.43	-3.08	-3.74	-4.94	-3.16

<sup>a</sup> $\Delta E_{\text{flat}}$  and  $\Delta E_{\text{edge}}$  denote the interaction energies of binding for “flat” and “edge” configurations, respectively, and  $\Delta \Delta E$  denotes the energy difference between them.

<sup>b</sup>“MM (before minimization)” denotes the MM calculations which are based on the QM predicted equilibrium structures without the energy minimization procedure (see Sec. II).

<sup>c</sup>“MM (after minimization)” denotes the MM calculations which are based on the structures initially derived from the QM predicted equilibrium structures and then slightly adjusted by the MM energy minimization procedures.

the equilibrium ring-CNT distance,  $d_{\text{equ}}$ . All MM predicted  $d_{\text{equ}}$  are found to be larger than the QM ones by a value of about 0.2 Å~0.4 Å (note that the DFTB-D predicted  $d_{\text{equ}}$  are about 0.2 Å~0.3 Å smaller than those of CHARMM). Remember that in case of benzene dimer with PD configuration, the DFTB-D method tends to underestimate the equilibrium distance (by 0.25 Å as compared to CCSD(T) value), whereas CHARMM’s result is more accurate (only an overestimation of 0.019 Å as compared to CCSD(T) value, see Table S3 in the supplementary material);<sup>82</sup> hence, it is quite plausible that  $d_{\text{equ}}$  predicted by MM approaches (especially for CHARMM case) in Table VI are more accurate than the DFTB-D predicted ones. Next, we use  $\theta$  (defined as the angle between long axes of the aromatic ring and the CNT, see Scheme 1) to characterize the binding pattern (matching surface). From Fig. 4 and Table VI, we can see that the QM and MM predicted structures are different in most cases. The principal exception is the structure of CHARMM Trp, which is very close to the corresponding QM predicted structure. It is interesting to find that in the QM equilibrium structure for Trp, the indole ring is perpendicular to the long axis of CNT ( $\theta \approx 90^\circ$ ), contrary to the intuition that it should be parallel to the long

TABLE V. Maximal induced charges on atoms of CNT and induction energies due to aromatic molecules-CNT binding.<sup>a</sup>

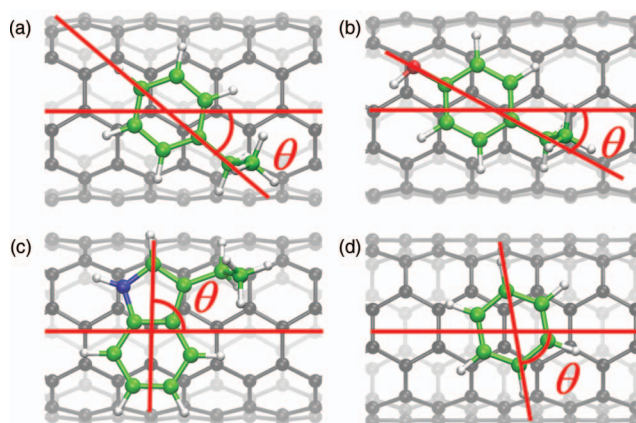
Induced charges and energies	Phe	Tyr	Trp	Ben
$Q_{\text{flat}} (\times 10^{-2} e)$	1.16	1.20	1.53	1.14
$Q_{\text{edge}} (\times 10^{-2} e)$	-0.157	-0.789	-1.68	-0.200
$E_{\text{induction}}^{\text{Flat}} (\times 10^{-2} \text{ kcal/mol})$	-1.52	-1.67	-4.65	-1.36
$E_{\text{induction}}^{\text{Edge}} (\times 10^{-2} \text{ kcal/mol})$	-0.0950	-1.24	-5.56	-0.110

<sup>a</sup> $Q$  denotes the induced charge with maximal absolute value (Mulliken charges determined by DFTB-D calculations) on atoms of CNT;  $E_{\text{induction}}$  denotes the induction energy between aromatic molecule and CNT due to binding. The subscripts (or superscripts) “flat” and “edge” are used to distinguish different configurations.

TABLE VI. Geometrical parameters of equilibrium binding structures for “flat” configuration.<sup>a</sup>

Geometry	DFTB-D	OPLSAA	AMBER	CHARMM	
Phe	$d_{\text{equ}}$	3.02	3.45	3.24	3.24
	$\theta$	41	4	60	56
Tyr	$d_{\text{equ}}$	3.02	3.40	3.36	3.32
	$\theta$	30	3	3	3
Trp	$d_{\text{equ}}$	3.02	3.36	3.25	3.21
	$\theta$	89	4	5	87
Benzene	$d_{\text{equ}}$	3.10	3.29	3.30	3.35
	$\theta$	80	64	57	80

<sup>a</sup> $d_{\text{equ}}$  (in Å) stands for the equilibrium ring-nanotube distance (see Fig. 3(a));  $\theta$  (in degree) is defined as the angle between long axes of the aromatic ring and the CNT (see Scheme 1).

SCHEME 1. Schematic representation of  $\theta$  used in Table VI for Phe, Tyr, Trp, and benzene [(a-d), respectively], using the QM predicted equilibrium structures for illustration.

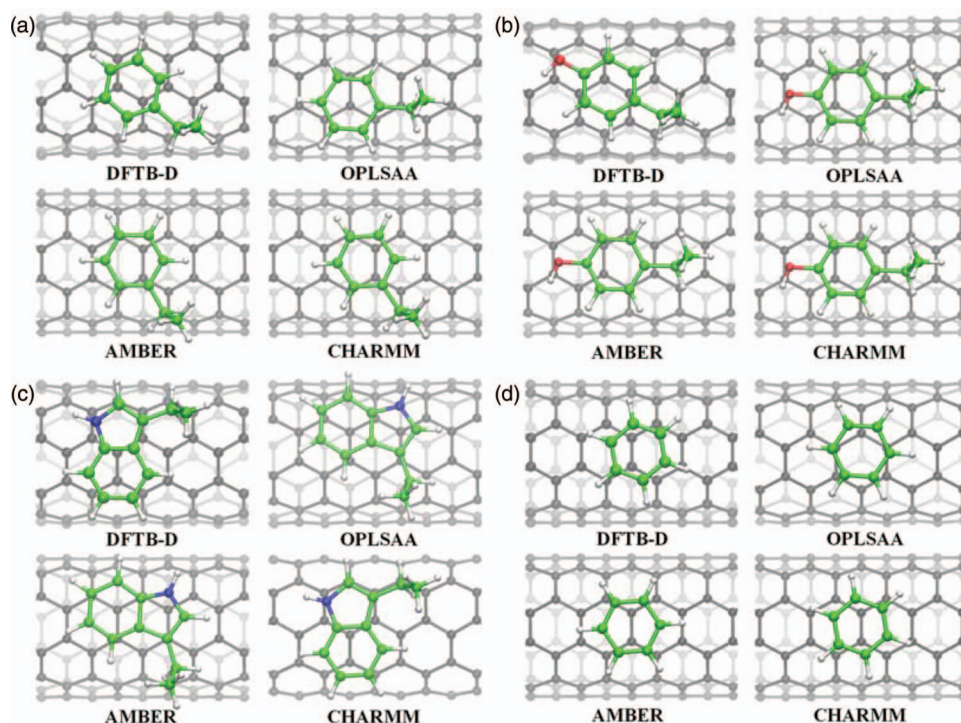


FIG. 4. Snapshots of the equilibrium structures predicted by different methods for Phe, Tyr, Trp, and benzene [(a–d), respectively] for “flat” configuration, shown in top view.

axis of CNT ( $\theta \approx 0^\circ$ ). In fact, the stable structure for Trp with  $\theta \approx 0^\circ$  exists in QM calculations, but it is about 0.13 kcal/mol less stable.

In the following, we discuss the QM predicted stacking geometries between aromatic rings of molecules and CNTs, in the hope that these results might provide useful benchmarks for future force field developments in addition to the above interaction energies. As shown in Fig. 4, the ring of aromatic molecule stacks over its nearest rings of CNT in an off-centered manner, consistent with previous studies of benzene dimer<sup>41–50</sup> and benzene-CNT complex,<sup>78–80</sup> which show that the off-centered geometry (slipped-parallel) of the stacked two aromatic rings is energetically more favorable than the “Sandwich” geometry. These off-centered geometries are similar to the “Bridge” and “Bridge-bis” geometries, following the nomenclature of Tournus and Charlier<sup>78</sup> for benzene adsorption on CNTs, which correspond to the structures that the carbon rings of molecules are exactly over a vertical and a biased carbon-carbon bonds (relative to CNT’s long axis), respectively. It is interesting to find that the carbon ring of benzene rotates a small angle relative to its nearest rings of CNT. These rotating angles are  $10^\circ$  (i.e.,  $90^\circ - \theta$ ) and  $11^\circ$  for benzene and Phe, respectively, whereas it is  $0^\circ$  for Tyr (see Figs. 3(a), 3(b), and 3(d)). To our knowledge, this rotatably stacked geometry is not reported by previous studies of benzene-CNT complex.<sup>78–81</sup>

#### IV. CONCLUSIONS

Most existing experimental evidences indicate that the most important driving forces for the binding of protein/peptide to pristine CNTs in aqueous solutions are the

hydrophobic interaction<sup>4,5,7,8,14–16</sup> and the  $\pi$ - $\pi$  stacking interaction,<sup>7,13,17–21</sup> although some other interactions, such as cation- $\pi$  interaction, may also play a role.<sup>6</sup> In practice, the CNTs usually have oxidized defects (commonly carboxylic group) or other added functional groups. When the pH value is below the isoelectric point, the electrostatic interaction between the protonated amine of protein/peptide and the carboxylic groups of CNT can then play a vital role in the binding process.<sup>5,18</sup> It has been widely accepted that MD simulations with fixed-charge force field (and explicit water) are capable of appropriately capturing the hydrophobic interaction and the electrostatic interaction, but their abilities to capture the  $\pi$ - $\pi$  stacking interactions are highly questioned by many researchers due to the lack of polarizability in these standard force fields.<sup>32,33,46</sup> In fact, it was suggested that MD simulations with fixed-charge force field may provide an insufficient description of the peptide-nanotube binding when the  $\pi$ - $\pi$  stacking interaction of aromatic residues with the nanotube is dominant.<sup>33</sup> However, the present work uses the DFTB-D method, which itself has been benchmarked with higher level quantum mechanical methods, to show that although the MM approaches with fixed-charge force fields may be incapable of predicting the exact binding structures, they can appropriately predict the strength of  $\pi$ - $\pi$  stacking interactions between aromatic molecules and CNTs, which is probably the most important aspect in the study of aromatic amino acids-CNT interactions. Also, we find that the CNT polarizability due to aromatic rings is negligible and the polarizable force fields might not be needed for studying  $\pi$ - $\pi$  interactions in this case. In view of the computational costs compared to QM calculations and MD simulations with polarizable force fields, it seems that MD simulations with fixed-charge force

fields provide a computationally efficient and reasonable way to study the protein/peptide-CNT interactions, including the  $\pi$ - $\pi$  (stacking) interactions. In addition, we have provided a comprehensive QM picture with various benchmarks for the  $\pi$ - $\pi$  interactions between small aromatic molecules as well as between aromatic molecules and CNTs in gas phase, which might be used as a benchmark for future force field developments.

## ACKNOWLEDGMENTS

We thank Xiaowei Tang, Weiqiu Zhu, Haiping Fang, Guanghong Zuo, Bo Zhou, Zhen Xia, Seung-gu Kang, and Payel Das for useful discussions and insightful comments. This work is partially supported by the National Natural Science Foundation of China (Grant Nos. 30870593 and 11004076), the China Postdoctoral Science Foundation (Grant No. 201104738), and the Fundamental Research Funds for the Central Universities. Z.W. acknowledges the High Performance Computing Center (HPCC) of Jilin University. R.Z. acknowledges the support from the IBM BlueGene Program.

- <sup>1</sup>A. A. Bhirde, V. Patel, J. Gavard, G. Zhang, A. A. Sousa, A. Masedunskas, R. D. Leapman, R. Weigert, J. S. Gutkind, and J. F. Rusling, *ACS Nano* **3**, 307 (2009).
- <sup>2</sup>S. Jain, V. S. Thakare, M. Das, A. K. Jain, and S. Patil, *Nanomedicine* **5**, 1277 (2010).
- <sup>3</sup>R. J. Chen, S. Bangsaruntip, K. A. Drouvalakis, N. W. S. Kam, M. Shim, Y. M. Li, W. Kim, P. J. Utz, and H. J. Dai, *Proc. Natl. Acad. Sci. U.S.A.* **100**, 4984 (2003).
- <sup>4</sup>W. F. DeGrado, G. Grigoryan, Y. H. Kim, R. Acharya, K. Axelrod, R. M. Jain, L. Willis, M. Drndic, and J. M. Kikkawa, *Science* **332**, 1071 (2011).
- <sup>5</sup>D. Nepal and K. E. Geckeler, *Small* **2**, 406 (2006).
- <sup>6</sup>D. Nepal and K. E. Geckeler, *Small* **3**, 1259 (2007).
- <sup>7</sup>S. Q. Wang, E. S. Humphreys, S. Y. Chung, D. F. Delduco, S. R. Lustig, H. Wang, K. N. Parker, N. W. Rizzo, S. Subramoney, Y. M. Chiang, and A. Jagota, *Nat. Mater.* **2**, 196 (2003).
- <sup>8</sup>G. R. Dieckmann, A. B. Dalton, P. A. Johnson, J. Razal, J. Chen, G. M. Giordano, E. Munoz, I. H. Musselman, R. H. Baughman, and R. K. Draper, *J. Am. Chem. Soc.* **125**, 1770 (2003).
- <sup>9</sup>V. E. Kagan, N. V. Konduru, W. H. Feng, B. L. Allen, J. Conroy, Y. Volkov, I. I. Vlasova, N. A. Belikova, N. Yanamala, A. Kapralov, Y. Y. Tyurina, J. W. Shi, E. R. Kisin, A. R. Murray, J. Franks, D. Stolz, P. P. Gou, J. Klein-Seetharaman, B. Fadeel, A. Star, and A. A. Shvedova, *Nat. Nanotechnol.* **5**, 354 (2010).
- <sup>10</sup>Y. L. Zhao, G. M. Xing, and Z. F. Chai, *Nat. Nanotechnol.* **3**, 191 (2008).
- <sup>11</sup>G. Zuo, W. Gu, H. Fang, and R. Zhou, *J. Phys. Chem. C* **115**, 12322 (2011).
- <sup>12</sup>G. Zuo, Q. Huang, G. Wei, R. Zhou, and H. Fang, *ACS Nano* **4**, 7508 (2010).
- <sup>13</sup>C. C. Ge, J. F. Du, L. N. Zhao, L. M. Wang, Y. Liu, D. H. Li, Y. L. Yang, R. H. Zhou, Y. L. Zhao, Z. F. Chai, and C. Y. Chen, *Proc. Natl. Acad. Sci. U.S.A.* **108**, 16968 (2011).
- <sup>14</sup>S. S. Karajanagi, A. A. Vertegel, R. S. Kane, and J. S. Dordick, *Langmuir* **20**, 11594 (2004).
- <sup>15</sup>P. Goldberg-Oppenheimer, and O. Regev, *Small* **3**, 1894 (2007).
- <sup>16</sup>J. Zhong, L. Song, J. Meng, B. Gao, W. Chu, H. Xu, Y. Luo, J. Guo, A. Marcelli, S. Xie, and Z. Wu, *Carbon* **47**, 967 (2009).
- <sup>17</sup>V. Zorbas, A. L. Smith, H. Xie, A. Ortiz-Acevedo, A. B. Dalton, G. R. Dieckmann, R. K. Draper, R. H. Baughman, and I. H. Musselman, *J. Am. Chem. Soc.* **127**, 12323 (2005).
- <sup>18</sup>X. J. Li, W. Chen, Q. W. Zhan, L. M. Dai, L. Sowards, M. Pender, and R. R. Naik, *J. Phys. Chem. B* **110**, 12621 (2006).
- <sup>19</sup>H. Xie, E. J. Becraft, R. H. Baughman, A. B. Dalton, and G. R. Dieckmann, *J. Pept. Sci.* **14**, 139 (2008).
- <sup>20</sup>Z. Su, K. Mui, E. Daub, T. Leung, and J. Honek, *J. Phys. Chem. B* **111**, 14411 (2007).
- <sup>21</sup>C. G. Salzmann, M. A. H. Ward, R. M. J. Jacobs, G. Tobias, and M. L. H. Green, *J. Phys. Chem. C* **111**, 18520 (2007).
- <sup>22</sup>T. Serizawa, Z. H. Gao, C. Y. Zhi, Y. Bando, and D. Golberg, *J. Am. Chem. Soc.* **132**, 4976 (2010).
- <sup>23</sup>J.-W. Shen, T. Wu, Q. Wang, and Y. Kang, *Biomaterials* **29**, 3847 (2008).
- <sup>24</sup>G. Gianese, V. Rosato, F. Cleri, M. Celino, and P. Morales, *J. Phys. Chem. B* **113**, 12105 (2009).
- <sup>25</sup>S. O. Nielsen, C. C. Chiu, and G. R. Dieckmann, *J. Phys. Chem. B* **112**, 16326 (2008).
- <sup>26</sup>M. S. P. Sansom, E. J. Wallace, R. S. G. D’Rozario, and B. M. Sanchez, *Nanoscale* **2**, 967 (2010).
- <sup>27</sup>C.-c. Chiu, M. C. Maher, G. R. Dieckmann, and S. O. Nielsen, *ACS Nano* **4**, 2539 (2010).
- <sup>28</sup>K. Balamurugan, R. Gopalakrishnan, S. S. Raman, and V. Subramanian, *J. Phys. Chem. B* **114**, 14048 (2010).
- <sup>29</sup>R. R. Johnson, B. J. Rego, A. T. C. Johnson, and M. L. Klein, *J. Phys. Chem. B* **113**, 11589 (2009).
- <sup>30</sup>Y. A. Cheng, D. C. Li, B. H. Ji, X. H. Shi, and H. J. Gao, *J. Mol. Graphics Modell.* **29**, 171 (2010).
- <sup>31</sup>Q. Wang, Y. Kang, Y. C. Liu, J. W. Shen, and T. Wu, *J. Phys. Chem. B* **114**, 2869 (2010).
- <sup>32</sup>T. R. Walsh, and S. D. Tomasio, *Mol. Phys.* **105**, 221 (2007).
- <sup>33</sup>T. R. Walsh, and S. M. Tomasio, *J. Phys. Chem. C* **113**, 8778 (2009).
- <sup>34</sup>S. Vaitheeswaran, and A. E. Garcia, *J. Chem. Phys.* **134**, 125101 (2011).
- <sup>35</sup>R. H. Zhou, X. H. Huang, C. J. Margulis, and B. J. Berne, *Science* **305**, 1605 (2004).
- <sup>36</sup>P. Liu, X. H. Huang, R. H. Zhou, and B. J. Berne, *Nature (London)* **437**, 159 (2005).
- <sup>37</sup>J. A. King, P. Das, and R. H. Zhou, *Proc. Natl. Acad. Sci. U.S.A.* **108**, 10514 (2011).
- <sup>38</sup>L. Zheng, M. Chen, and W. Yang, *Proc. Natl. Acad. Sci. U.S.A.* **105**, 20227 (2008).
- <sup>39</sup>H. Kamberaj and A. van der Vaart, *J. Chem. Phys.* **130**, 074906 (2009).
- <sup>40</sup>R. R. Johnson, A. Kohlmeier, A. T. C. Johnson, and M. L. Klein, *Nano Lett.* **9**, 537 (2009).
- <sup>41</sup>S. Tsuzuki, K. Honda, T. Uchimaru, M. Mikami, and K. Tanabe, *J. Am. Chem. Soc.* **124**, 104 (2002).
- <sup>42</sup>E. C. Lee, D. Kim, P. Jurecka, P. Tarakeswar, P. Hobza, and K. S. Kim, *J. Phys. Chem. A* **111**, 3446 (2007).
- <sup>43</sup>M. Pitonak, P. Neogrady, J. Rezac, P. Jurecka, M. Urban, and P. Hobza, *J. Chem. Theory Comput.* **4**, 1829 (2008).
- <sup>44</sup>M. Lewis, M. W. Watt, M. L. K. E. Hardebeck, and C. C. Kirkpatrick, *J. Am. Chem. Soc.* **133**, 3854 (2011).
- <sup>45</sup>C. D. Sherrill and M. O. Sinnokrot, *J. Phys. Chem. A* **110**, 10656 (2006).
- <sup>46</sup>C. D. Sherrill, B. G. Sumpter, M. O. Sinnokrot, M. S. Marshall, E. G. Hohenstein, R. C. Walker, and I. R. Gould, *J. Comput. Chem.* **30**, 2187 (2009).
- <sup>47</sup>S. Grimme, *J. Comput. Chem.* **25**, 1463 (2004).
- <sup>48</sup>P. Jurecka, J. Sponer, J. Cerny, and P. Hobza, *Phys. Chem. Chem. Phys.* **8**, 1985 (2006).
- <sup>49</sup>M. O. Sinnokrot and C. D. Sherrill, *J. Phys. Chem. A* **108**, 10200 (2004).
- <sup>50</sup>T. Janowski and P. Pulay, *Chem. Phys. Lett.* **447**, 27 (2007).
- <sup>51</sup>Y. Zhao and D. G. Truhlar, *J. Phys. Chem. C* **112**, 4061 (2008).
- <sup>52</sup>W. L. Jorgensen and D. L. Severance, *J. Am. Chem. Soc.* **112**, 4768 (1990).
- <sup>53</sup>C. Chipot, R. Jaffe, B. Maignet, D. A. Pearlman, and P. A. Kollman, *J. Am. Chem. Soc.* **118**, 11217 (1996).
- <sup>54</sup>A. T. Macias and A. D. MacKerell, *J. Comput. Chem.* **26**, 1452 (2005).
- <sup>55</sup>Y. P. Pang, J. L. Miller, and P. A. Kollman, *J. Am. Chem. Soc.* **121**, 1717 (1999).
- <sup>56</sup>W. D. Cornell, P. Cieplak, C. I. Bayly, I. R. Gould, K. M. Merz, D. M. Ferguson, D. C. Spellmeyer, T. Fox, J. W. Caldwell, and P. A. Kollman, *J. Am. Chem. Soc.* **117**, 5179 (1996).
- <sup>57</sup>A. de Leon, A. F. Jalbout, and V. A. Basiuk, *Chem. Phys. Lett.* **457**, 185 (2008).
- <sup>58</sup>A. F. Jalbout, A. De Leon, and V. A. Basiuk, *Comp Mater Sci* **44**, 310 (2008).
- <sup>59</sup>R. Sharma, J. P. McNamara, R. K. Raju, M. A. Vincent, I. H. Hillier, and C. A. Morgado, *Phys. Chem. Chem. Phys.* **10**, 2767 (2008).
- <sup>60</sup>W. Fan, J. Zeng, and R. Zhang, *J. Chem. Theory Comput.* **5**, 2879 (2009).
- <sup>61</sup>M. Elstner, D. Porezag, G. Jungnickel, J. Elsner, M. Haugk, T. Frauenheim, S. Suhai, and G. Seifert, *Phys. Rev. B* **58**, 7260 (1998).
- <sup>62</sup>B. Aradi, B. Hourahine, and T. Frauenheim, *J. Phys. Chem. A* **111**, 5678 (2007).

- <sup>63</sup>M. Elstner, P. Hobza, T. Frauenheim, S. Suhai, and E. Kaxiras, *J. Chem. Phys.* **114**, 5149 (2001).
- <sup>64</sup>W. L. Jorgensen, D. S. Maxwell, and J. TiradoRives, *J. Am. Chem. Soc.* **118**, 11225 (1996).
- <sup>65</sup>J. M. Wang, P. Cieplak, and P. A. Kollman, *J. Comput. Chem.* **21**, 1049 (2000).
- <sup>66</sup>A. D. Mackerell, M. Feig, and C. L. Brooks, *J. Comput. Chem.* **25**, 1400 (2004).
- <sup>67</sup>P. Hobza, J. Sponer, and T. Reschel, *J. Comput. Chem.* **16**, 1315 (1995).
- <sup>68</sup>Y. Zhao, X. Wu, J. Yang, and X. C. Zeng, *Phys. Chem. Chem. Phys.* **13**, 11766 (2011).
- <sup>69</sup>L. Zhechkov, T. Heine, S. Patchkovskii, G. Seifert, and H. A. Duarte, *J. Chem. Theory Comput.* **1**, 841 (2005).
- <sup>70</sup>J. R. Grover, E. A. Walters, and E. T. Hui, *J. Phys. Chem.* **91**, 3233 (1987).
- <sup>71</sup>Elkingto. Pa and G. Curthoys, *J. Phys. Chem.* **73**, 2321 (1969).
- <sup>72</sup>E. Arunan and H. S. Gutowsky, *J. Chem. Phys.* **98**, 4294 (1993).
- <sup>73</sup>B. Hess, C. Kutzner, D. van der Spoel, and E. Lindahl, *J. Chem. Theory Comput.* **4**, 435 (2008).
- <sup>74</sup>W. Humphrey, A. Dalke, and K. Schulten, *J. Mol. Graphics* **14**, 33 (1996).
- <sup>75</sup>G. Hummer, J. C. Rasaiah, and J. P. Noworyta, *Nature (London)* **414**, 188 (2001).
- <sup>76</sup>P. Xiu, B. Zhou, W. P. Qi, H. J. Lu, Y. S. Tu, and H. P. Fang, *J. Am. Chem. Soc.* **131**, 2840 (2009).
- <sup>77</sup>P. Xiu, Z. X. Yang, B. Zhou, P. Das, H. P. Fang, and R. H. Zhou, *J. Phys. Chem. B* **115**, 2988 (2011).
- <sup>78</sup>F. Tournus, and J. C. Charlier, *Phys. Rev. B* **71**, 165421 (2005).
- <sup>79</sup>L. M. Woods, S. C. Badescu, and T. L. Reinecke, *Phys. Rev. B* **75**, 155415 (2007).
- <sup>80</sup>J. P. Lu, J. J. Zhao, J. Han, and C. K. Yang, *Appl. Phys. Lett.* **82**, 3746 (2003).
- <sup>81</sup>J. Lu, S. Nagase, X. W. Zhang, D. Wang, M. Ni, Y. Maeda, T. Wakahara, T. Nakahodo, T. Tsuchiya, T. Akasaka, Z. X. Gao, D. P. Yu, H. Q. Ye, W. N. Mei, and Y. S. Zhou, *J. Am. Chem. Soc.* **128**, 5114 (2006).
- <sup>82</sup>See supplementary material at <http://dx.doi.org/10.1063/1.3675486> for analysis of interaction energies of benzene dimer with different configurations for OPLSAA and CHARMM force fields, complete lists of interaction energies and equilibrium distances of benzene dimer obtained by different methods, nonbonded parameters for aromatic amino acid analogues in MM calculations, snapshots of equilibrium binding structures predicted by QM calculations, and comparison of equilibrium binding structures predicted by QM and MM calculations for the “edge” configuration.